Surface Oxide and the Role of Magnesium during the Sintering of Aluminum

R.N. LUMLEY, T.B. SERCOMBE, and G.B. SCHAFFER

The effect of trace additions of magnesium on the sintering of aluminum and its alloys is examined. Magnesium, especially at low concentrations, has a disproportionate effect on sintering because it disrupts the passivating Al_2O_3 layer through the formation of a spinel phase. Magnesium penetrates the sintering compact by solid-state diffusion, and the oxide is reduced at the metal-oxide interface. This facilitates solid-state sintering, as well as wetting of the underlying metal by sintering liquids, when these are present. The optimum magnesium concentration is approximately 0.1 to 1.0 wt pct, but this is dependent on the volume of oxide and, hence, the particle size, as well as the sintering conditions. Small particle-size fractions require proportionally more magnesium than large-size fractions do.

I. INTRODUCTION

MOST metal powders exposed to oxygen are covered by a surface oxide layer. This oxide prevents solid-state sintering in low-melting-point metals,[1] including aluminum,[2] but not in all metals.[3,4,5] This has been explained in terms of the relative diffusion rates through the oxide and the metal, for metals with stable oxides.[6,7] The oxide on aluminum, therefore, needs to be reduced or otherwise removed to enable effective sintering. The oxidation of a metal (M) may be represented by

$$M + O_2 \leftrightarrow MO_2 \quad [1]$$

The free energy of formation (ΔG) of the oxide is given by

$$\Delta G = -RT \ln K_1 \quad [2]$$

where R is the gas constant, T is the temperature in Kelvin, and K_1 is the equilibrium constant given by

$$K_1 = (P_{O_2})^{-1} \quad [3]$$

where P_{O_2} is the partial pressure of oxygen when reaction [1] is at equilibrium. For aluminum at 600 °C, a $P_{O_2} < 10^{-50}$ atm is required to reduce the oxide.[8] Atmospheres containing hydrogen are often used in powder metallurgy. Hydrogen can reduce a metal oxide by the reaction

$$MO + H_2 \leftrightarrow M + H_2O \quad [4]$$

The equilibrium constant for this reaction (K_4) is given by

$$K_4 = P_{H_2O}/P_{H_2} \quad [5]$$

where P_{H_2} and P_{H_2O} are the partial pressure of hydrogen and water vapor, respectively. The ratio of partial pressures can be converted to the dew point, which is effectively the water vapor content. A dew point of ≤−140 °C at 600 °C is required to reduce Al_2O_3.[9] Neither a dew point of −140 °C nor a P_{O_2} of 10^{-50} atm is physically attainable, and, therefore, aluminum cannot be sintered in conventional atmospheres.

The use of liquid phases is an alternative to solid-state sintering. An essential requirement for effective liquid-phase sintering is a wetting liquid.[10] The wettability of a solid by a liquid is determined by the work of adhesion (W_a):[11,12]

$$W_a = \gamma_{lv}(1 + \cos\theta) = \gamma_{sv} + \gamma_{lv} - \gamma_{sl} \quad [6]$$

where γ_{lv} is the surface tension of the liquid, γ_{sv} is the surface tension of the solid-vapor interface, γ_{sl} is the solid-liquid interfacial tension, and θ is the contact angle. A liquid is said to wet a solid when $\cos\theta > 0$. High-melting-point metal oxides are generally poorly wetted by liquid metals, except above the wetting threshold, a temperature beyond which W_a increases sharply.[11] Liquid aluminum is not, therefore, expected to wet alumina near the melting point of the metal. Indeed, the contact angle is variously given as ~103 deg at 900 °C,[13] ~160 deg at 800 °C,[14] or ~162 deg at 950 °C,[15] although this is dependent on the partial pressure of oxygen and the presence of an oxide film on the molten metal.[16] It has been suggested that the Al-$CuAl_2$ eutectic can wet Al_2O_3 at 600 °C.[17] However, neither Mg, Ce, nor Ca additions to molten Al reduce the contact angle sufficiently to produce wetting.[13,14] Since the work of adhesion of liquid metals on oxide surfaces increases with the free energy of formation of the metal oxide,[18] it is unlikely that Cu will be efficacious.

It is, thus, apparent that the sesquioxide is an obstruction which must be disrupted to facilitate sintering. Here, we examine the sintering of aluminum and its alloys with separate trace additions of elemental magnesium and propose a mechanism by which magnesium ruptures the oxide, thereby allowing effective sintering to occur.

II. EXPERIMENTAL PROCEDURE

All alloys were made from mixtures of elemental powders. The starting powder characteristics are presented in Table I. All powder had a purity >99.5 pct. The coarser aluminum powder (No. 2) was used throughout, except in the zinc ternary system and in the powder prepared for transmission electron microscopy (TEM) analysis, where

R.N. LUMLEY and T.B. SERCOMBE, Postgraduate Students, and G.M. SCHAFFER, Senior Lecturer, are with the Department of Mining, Minerals and Materials Engineering, The University of Queensland, QLD 4072, Australia.

Manuscript submitted December 5, 1997.

Table I. Starting Powder Characteristics

Powder	Fabrication Method	Powder Shape	Powder Sizes	Source
Aluminum 1	air atomized	ligamental	0 to 1 pct −250 +150 μm 35 to 55 pct −150 +63 μm bal −63 +45 μm 32 to 52 pct −45 μm	Comalco Aluminum Ltd.
Aluminum 2	air atomized	ligamental	0 to 2 pct −250 +150 μm bal −150 +75 μm 25 to 50 pct −75 +45 μm 32 to 52 pct −45 μm	Comalco Aluminum Ltd.
Magnesium	mechanical	flake	−45 μm	Cerac Inc.
Tin	air atomized		0 to 5 pct −106 +75 μm 20 pct max −75 +45 μm 15 pct max −45 +38 μm 65 to 85 pct −38 μm	ACL Bearing Co.
Zinc	air atomized	ligamental	trace >355 μm 25 pct >150 μm 37 pct >106 μm 71 pct >63 μm 96 pct >45 μm 4 pct <45 μm	Pometon SpA

Table II. The Alloy Systems Investivated

	Composition (Wt Pct)			
Alloy System	Mg	Sn	Zn	Al
Al-Mg	0 to 2.5	—	—	bal
Al-Sn	0 to 1.5	8	—	bal
Al-Zn	0 to 0.2	—	8	bal

aluminum powder No. 1 was used. The composition ranges of the alloy systems investigated are presented in Table II. The Al-Zn-Mg system had 0.5 pct stearic acid added as a lubricant; all other alloys had 1 pct additions (all compositions in wt pct). Mixing was conducted in a Turbula powder mixer for 20 to 30 minutes. Specimens weighed 3 to 5 g and were uniaxially cold pressed in a floating die into either a bar (~40 × ~9 mm) or a cylinder (ϕ = 14.34 mm). Compaction pressure ranged from 200 to 400 MPa. To remove the lubricant, samples were dewaxed at temperatures from 200 °C to 300 °C for up to 30 minutes.[19] Sintering was conducted in a high-purity nitrogen atmosphere with a dew point of ≤−40 °C, at temperatures between 550 °C and 620 °C. Heating rates of 10 °C to 20 °C/min were used. Specific compositions and process conditions are detailed in the figure captions.

Samples were prepared for microstructural analysis using standard polishing methods and were finished on 0.05 μm silica. These were etched in 0.5 vol pct HF for optical metallography. Compacts for scanning electron microscopy analysis were unetched and examined in a JEOL* 6400F scanning electron microscope. The TEM samples were prepared using the window technique in a solution of 10 pct perchloric acid in methanol at ~0 °C and were examined in a JEOL 4000T at 400 keV. Both electron microscopes were equipped with windowless Link energy-dispersive spectroscopy (EDS) facilities. Dilatometry was conducted using a Netzsch DIL 402C instrument under dried, high-purity nitrogen. Surface-area analysis was performed on a Micromeritics Gemini 2375 instrument, using a 5-point BET model. Five equispaced relative pressures were used, ranging between 0.05 and 0.3. A free-space correction using helium was also incorporated. Oxide thickness was determined by electron spectroscopy for chemical analysis (ESCA) using a PHI 560 ESCA/SAM/SIMS 1 multitechnique system incorporating a 25-270AR cylindrical mirror analyser.

*JEOL is a trademark of Japan Electron Optics Ltd., Tokyo.

The sample hardness was determined by taking the average of at least five separate indentations using a Buehler Rockwell hardness tester. Tensile properties were determined using an Instron 1026 screw-drive tensile machine with a 10 kN load cell and a crosshead speed of 0.6 mm/min. Strain was measured by an Instron model 2620/603 dynamic extensometer with a full-scale range of 20 pct. Sintered density measurements were obtained by following the MPIF standard 42, except that ethanol was used instead of water. The change in density is reported as the densification (φ), as follows:

$$\varphi = (\rho_s - \rho_g)/(\rho_t - \rho_g) \quad [7]$$

where ρ_s is the sintered density, ρ_g is the green density, and ρ_t is the theoretical density.

III. RESULTS

The effect of small additions of magnesium on the sintering response of aluminum is apparent from the dilatometry, for which a solid, pure aluminum pellet was used as a standard (Figure 1). There is no significant difference between the solid standard and pressed aluminum powder. When Mg is added to Al powder, expansion begins at ~275 °C, and there is a second dilation at ~500 °C in the Al-1.5Mg alloy. The addition of some magnesium causes shrinkage during sintering, and it is apparent from the densification curve of Figure 2 that the shrinkage is maximized at 0.15 pct Mg. Additions greater than 1 pct cause net expansion. Similar effects occur in the Al-8Sn system: the maximum densification again occurs at 0.15 pct Mg, where

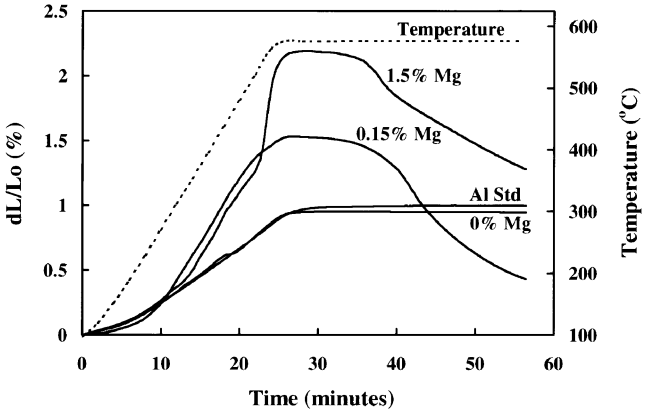

Fig. 1—Dilatometry curves for Al-*x*Mg alloys, where *x* is 0, 0.15, and 1.5 wt pct Mg showing the effect of trace additions of magnesium on the sintering response of aluminum. The powder was compacted at 200 MPa, dewaxed at 200 °C prior to dilatometry, and heated at 20 °C/min to a sintering temperature of 580 °C.

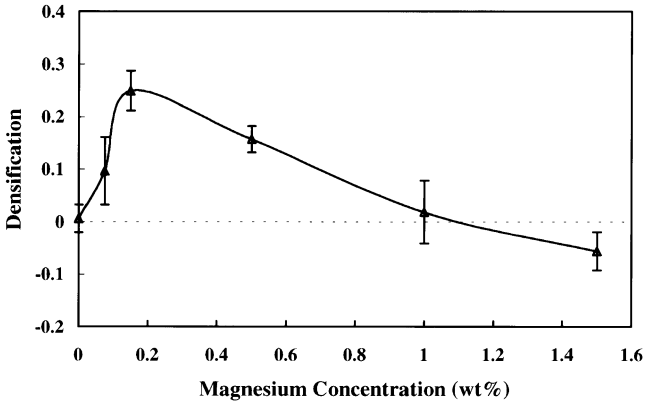

Fig. 2—The effect of magnesium on the densification of aluminum powder. The densification is maximized at 0.15 pct Mg, and there is net expansion at concentrations > 1 pct (the densification is defined by Eq. [7]; positive numbers indicate shrinkage). The samples were pressed at 200 MPa, dewaxed at 200 °C, heated at 20 °C/min, sintered at 620 °C for 30 min, and air cooled.

the sintered density reaches 99 pct of the theoretical density. The microstructures of Al-8Sn with and without Mg are compared in Figure 3. Liquid tin only wets aluminum in the presence of magnesium, when the dihedral angles are very sharp. Without magnesium, liquid tin is exuded from the sample during sintering. The Al-8Zn system also shows a similar response on the addition of magnesium. Optical microstructures for this system are presented in Figure 4. Increasing magnesium levels decreased the amount of liquid which formed and the duration for which it persisted. In contrast to the zero-magnesium sample, the liquid phase in the 0.2 pct Mg sample spreads beyond the prior-zinc particle sites.

The tensile properties correspond to these microstructural changes (Figure 5). In both the Al-*x*Mg and Al-8Sn-*x*Mg systems, the ductility passes through a maximum at 0.15 pct Mg. The tensile strength increases with increasing magnesium concentration, although the effect is greater at a magnesium concentration ≤0.15 pct. Similarly, the hardness of the Al-8Zn-*x*Mg alloys increases with magnesium.

While the microstructure of the binary Al-Mg alloys was largely homogeneous, TEM identified occasional second-phase regions. These consisted of fine crystals (Figure 6) which were enriched in magnesium and oxygen (Figure 7). The diffraction rings from this region could be indexed to spinel ($MgAl_2O_4$). However, γ-Al_2O_3 is isostructural with spinel and they share the same space group ($Fd3m$). The lattice parameters are also very similar: 7.90 Å for γ-alumina and 8.08 Å for spinel.[20] It is, therefore, not possible to differentiate γ-alumina from spinel by the electron diffraction pattern alone. Because the amorphous oxide which forms on the aluminum dehydrates and transforms to γ-alumina by 500 °C,[21–24] it is possible that these fine crystallites are alumina. However, the substantial magnesium presence, apparent in the EDS spectrum, indicates that this phase is more likely to be spinel.

The ESCA indicated that the oxide thickness was approximately 50 Å, and is independent of particle size,[25] which is consistent with similar work reported elsewhere.[26] The surface area of selected aluminum powders is given in Table III. The volume of the oxide layer is, then, simply the product of the thickness and the surface area.

IV. DISCUSSION

It is apparent from the accumulated evidence presented here that small quantities of magnesium have a significant effect on the sintering response of aluminum and its alloys and on the resulting mechanical properties. Previous studies have also shown that the sintering of aluminum is enhanced in the presence of magnesium, although neither direct experimental evidence nor a mechanism was provided.[27,28,29] It has also been shown that a magnesium source in a nitrogen atmosphere enhances sintering at low green densities through the formation of Mg_3N_2 vapor.[30] More recently, X-ray photoelectron spectroscopy indicated that the surface oxide can be reduced in the presence of magnesium, which exposes fresh metal and facilitates the subsequent formation of AIN on exposed surfaces.[31] Here, we consider how magnesium influences the sintering of oxide-covered aluminium powder.

Wetting occurs during sintering in the presence of magnesium (Figure 3); yet, the liquids present during sintering are unlikely to wet the oxide skin. This indicates that the liquid is probably in contact with the underlying aluminum metal and that the oxide skin had been ruptured. Some rupture of the oxide occurs during compaction, when it is fractured by shear.[32–36] However, shear during compaction as the only rupture mechanism is insufficient for effective sintering; otherwise, the Al-Sn system, which had been pressed to a green density of 95 pct, would not exude liquid metal. This indicates that an additional mechanism is operative and that magnesium is also involved in oxide rupture. Magnesium is highly reactive, and the free energy of formation of its oxide is more negative than that of the oxides of aluminum.[36] Magnesium, therefore, has the potential to act as a solid-reducing agent in this system. This suggests that the magnesium could reduce the aluminum sesquioxide, rupturing the oxide film sufficiently to facilitate diffusion, wetting, and sintering. That spinel is observed after sintering is an indication that these reduction reactions do, indeed, occur. The phase change may be accompanied by a change in volume, creating shear stresses

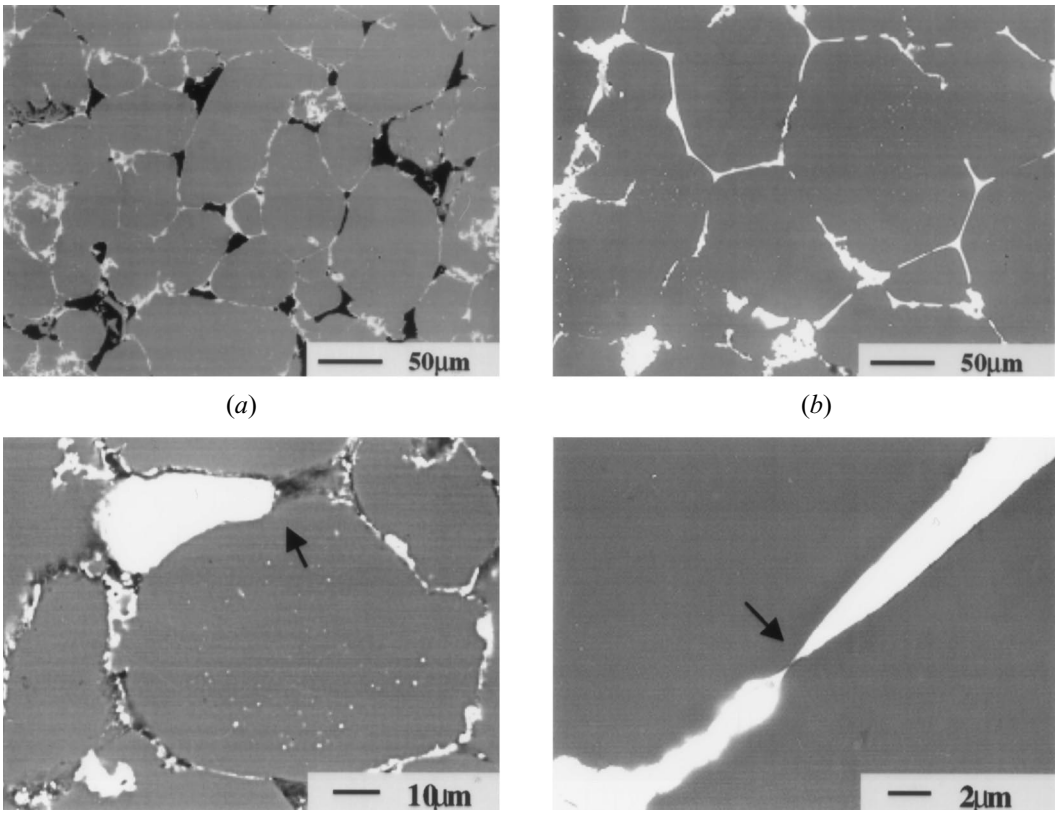

Fig. 3—Typical backscattered SEM micrographs of Al-8Sn-*x*Mg, where *x* equals 0 in (*a*) and (*c*) or 0.15 in (*b*) and (*d*). The white phase is tin, the gray phase is aluminum, and the black regions are pores. The Sn is poorly distributed over particle boundaries in (a) and is well distributed in (b), where the porosity is also reduced. The Sn-Al contact angle (arrowed) is large in (c) but small in (d). By eliminating the oxide as a barrier, magnesium reduces the contact angle, which facilitates wetting and improves sintering. The samples were pressed at 200 MPa, dewaxed at 200 °C, heated at 20 °C/min, sintered at 620 °C for 30 min, and air cooled.

in the film, ultimately leading to its break-up. This will create sites for liquid penetration, and sintering can then occur by the normal liquid-phase mechanisms.

A potential problem with the hypothesis that magnesium is the causal agent for oxide rupture is the dual observation that low concentrations of magnesium are required and that these reactions occur extensively at relatively low temperatures. This raises the question as to how the magnesium is adequately dispersed through the system in the presence of the oxide and before significant liquid-phase formation occurs. The presence of spinel, as opposed to magnesium oxide, suggests an explanation. A possible reaction for the formation of spinel is

$$3Mg + 4Al_2O_3 \leftrightarrow 3MgAl_2O_4 + 2Al \qquad [8]$$

which is a partial reduction reaction. Reaction [8] is observed at bonding interfaces in metal matrix composites[38–43] and in studies of the oxidation behavior of Al-Mg alloys.[21,44] At concentrations between 4 and 8 pct Mg in Al-Mg based composites, complete reduction is favored:

$$3Mg + Al_2O_3 \leftrightarrow 3\ MgO + 2Al \qquad [9]$$

as indicated by analysis of the equilibrium activity of Mg.[38] Because of the relative changes in free energy, reaction [8] is favored at low magnesium levels. McLeod and Gabryel[43] calculated the Mg concentration in equilibrium with reactions [8] and [9] and suggested that as little as 0.01 pct Mg is required to facilitate reaction [8] in the solid state.

The presence of spinel in Al-Mg powder alloys, therefore, indicates that the local Mg concentration may have been low when oxide rupture occurred. In contrast, MgO should occur if the reaction proceeded *via* direct contact with Mg particles or with the Al-Mg eutectic liquid. However, no evidence for MgO was found. This suggests that the oxide was not reduced through contact with the eutectic liquid. Furthermore, it is unnecessary for the magnesium to be in contact with the exterior of the powder particles; there is no apparent reason why the oxide could not be reduced from within. Some direct Al-Mg contact will be established during compaction. The magnesium could diffuse through the aluminum and along the aluminum-oxide interface from these contact points and react at the metal-oxide interface, not at the oxide-vapor interface. In this way, only a limited quantity of magnesium is required, as observed experimentally. This also facilitates reaction in the solid state at temperatures below the eutectic temperature.

A possible sequence of events in the disruption of the oxide is as follows:

(1) local oxide regions are ruptured during compaction, forming Al-Mg contact sites;
(2) MgO may form where Mg is in direct contact with Al_2O_3, although no evidence for this reaction was found;

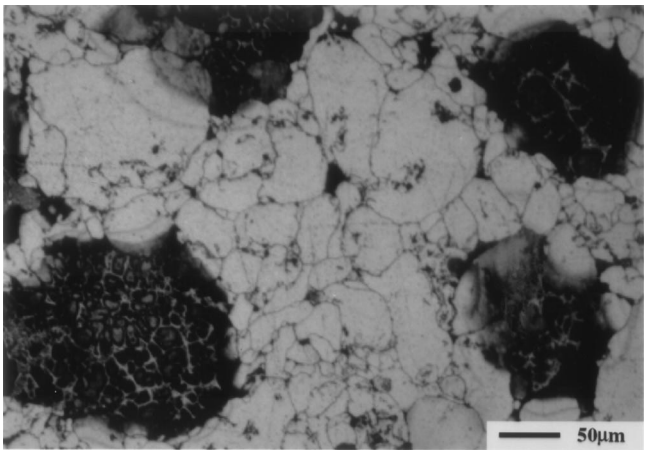

(*a*)

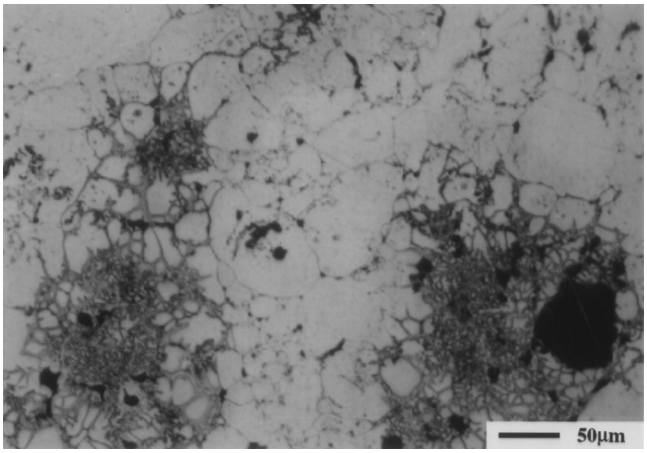

(*b*)

Fig. 4—Typical optical micrographs of Al-8Zn-*x*Mg: (*a*) $x = 0$ pct and (*b*) $x = 0.2$ pct. The gray phase is aluminum and the dark phase is Zn-Al eutectic. The samples were pressed at 250 MPa, dewaxed at 300 °C, heated at 10 °C/min, and quenched into water from 600 °C.

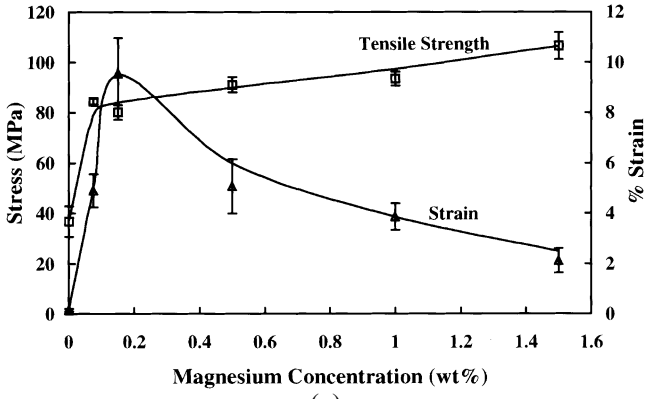

(*a*)

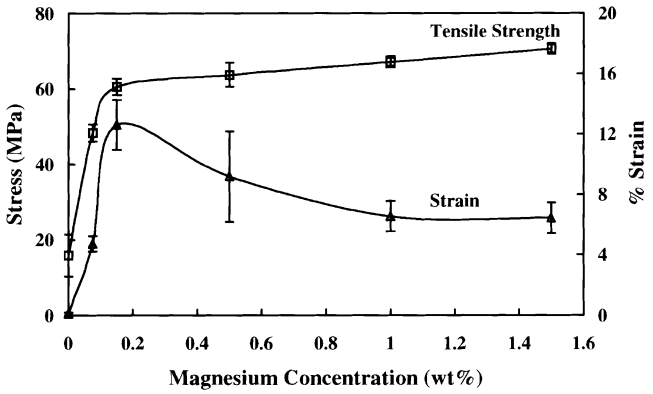

(*b*)

Fig. 5—The effect of magnesium on the tensile properties of (*a*) Al-*x*Mg and (*b*) Al-8Sn-*x*Mg. The properties in both systems are maximized at 0.15 pct Mg. The samples were pressed at 200 MPa, dewaxed at 200 °C, heated at 20 °C/min, sintered at 620 °C for 30 min, and air cooled.

(3) the magnesium diffuses along the metal-oxide interface and through the aluminum powder from the Al-Mg contact points established during compaction;
(4) magnesium reduces the oxide at the metal-oxide interface, forming spinel;
(5) nearby aluminum particles, which were not directly in contact with magnesium powder, are subsequently exposed to the reductant and their oxide layers are disrupted.

This is presented schematically in Figure 8. In this way the magnesium, even at low concentrations, can chemically attack the aluminum oxide layer and disrupt it sufficiently to allow an improved sintering response.

If the magnesium hypothesis is correct, then the critical concentration should vary with oxide volume and, hence, particle size. In order to test the hypothesis, aluminum powder was sieved to produce three specific size fractions. These were -38 μm, -125 $+75$ μm, and -212 $+150$ μm. The surface area and oxide volume for these powders are given in Table III. The sieved aluminum powder was sintered at 620 °C for 30 minutes with varying amounts of magnesium. The optimum magnesium concentration for maximum densification for each size fraction could then be determined. This is presented in Figure 9 as a function of particle size and oxide volume. The critical magnesium level* increases monotonically with oxide volume and, hence, decreases with particle size, as predicted. Given the oxide volume (Table III),it is possible to calculate the mass of oxide per gram of aluminum in the as-received powder and, hence, the amount of magnesium required for Eq. [8] to go to completion. The theoretical magnesium concentration for aluminum powder No. 2 is 0.05 pct, which is one-third of that found experimentally. That excess magnesium is required is not surprising, since some will react with the lubricant to form magnesium stearate and some will remain in solid solution in the aluminum.

*The critical magnesium level is greater than that determined for aluminum powder No. 2, because the compacts for this series of experiments were dewaxed at 300 °C rather than at 200 °C, and more magnesium stearate would have formed prior to sintering, reducing the amount of free magnesium.

Magnesium-induced oxide rupture can explain the various expansion and shrinkage events in the dilatometry of Figure 1, the form of the densification curves in Figure 2, and the mechanical property curves of Figure 5. The first dilation (Figure 1), at 275 °C in the magnesium-containing alloys, is due to the Kirkendall effect.[45] This is indicative of at least some oxide rupture. Shrinkage ultimately occurs after an incubation period at the sintering temperature, when sufficient oxide has been reduced. The sample without magnesium does not densify. The second dilation, at

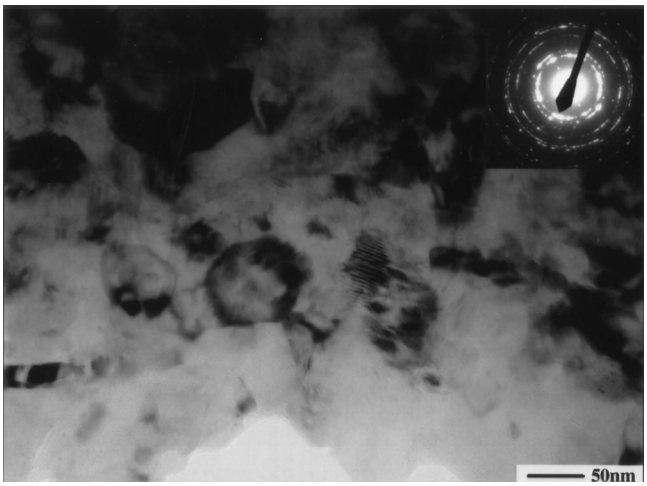

Fig. 6—Many beam TEM micrograph of a sintered Al-2.5 pct Mg alloy, showing a multitude of spinel crystallites. The inset shows the selected area diffraction pattern from this region; it can be indexed to spinel. The sample was pressed at 400 MPa, dewaxed at 200 °C, heated at 10 °C/min to 550 °C, and air cooled.

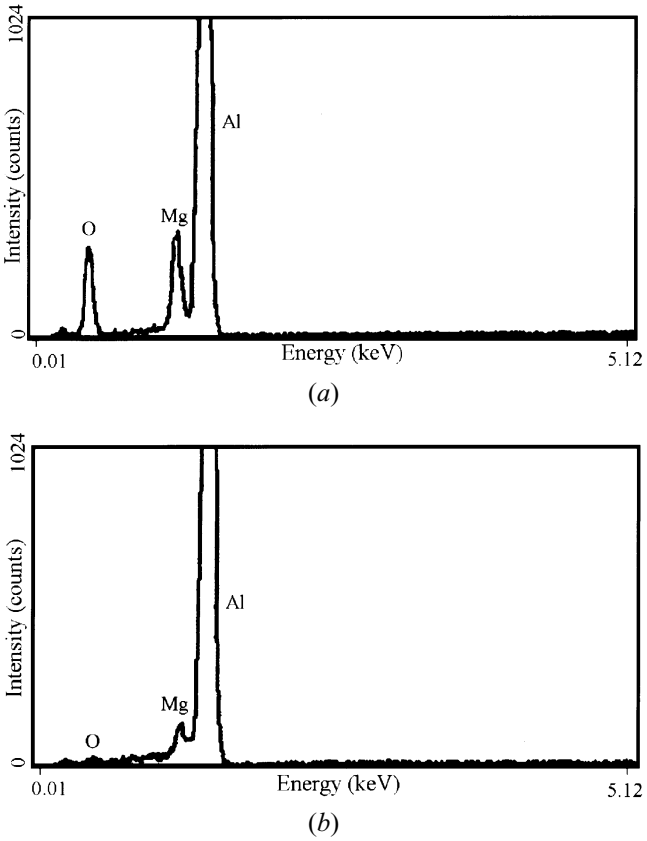

Fig. 7—EDS spectra from (*a*) the spinel region in Fig. 6 and (*b*) the adjacent aluminum, showing that the fine crystallites contain significantly more magnesium and oxygen than does the aluminum matrix.

~500 °C in the high-magnesium alloy, is a result of eutectic liquid formation. It is apparent that the eutectic forms after oxide breakup and will result from a reaction between the excess magnesium and the aluminum. That the eutectic liquid forms at ~50 °C above the equilibrium temperature may be a consequence of thermal lag and severe nonequilibrium. The densification curve (Figure 2) for the binary

Table III. Surface Area and Oxide Volume for Selected Aluminum Powders

Powder	BET Surface Area (m^2/g)	Oxide Volume (10^{-10} m^3/g)
Aluminum 2	0.14	7.2
< 38 μm	0.31	15.8
−125 + 75 μm	0.16	8.3
−212 + 150 μm	0.11	5.8

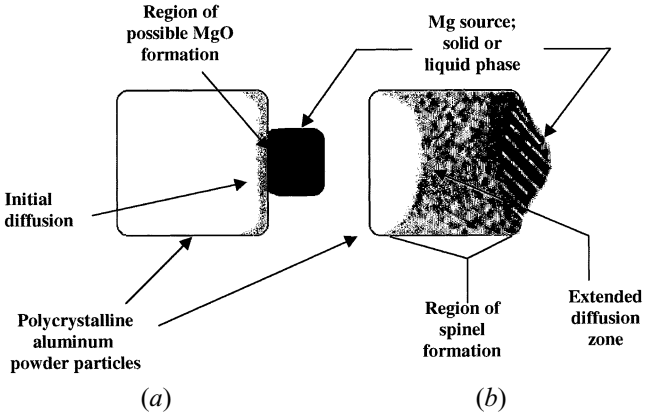

Fig. 8—(*a*) and (*b*) A schematic representation of the processes involved in the reduction of the alumina layer by magnesium during the sintering of Al-Mg alloys.

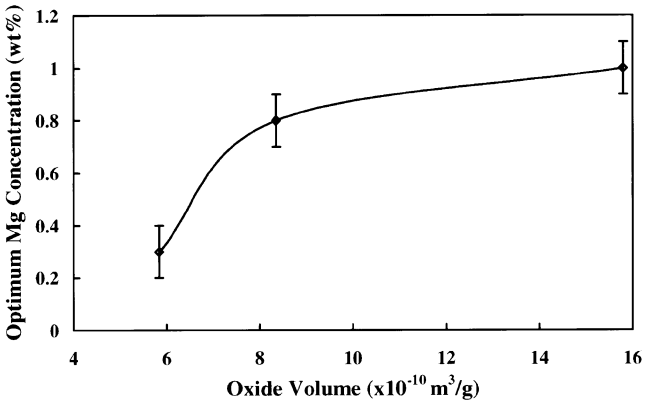

Fig. 9—The concentration of magnesium required to achieve maximum densification in a binary Al-Mg alloy as a function of oxide volume for three discrete particle sizes showing that more magnesium is required to sinter small powders because of the greater relative amount of oxide. The samples were pressed to a green density of 91 ± 0.5 pct, dewaxed at 300 °C, heated at 20 °C/min to 620 °C for 30 min, and air cooled.

alloy shows a peak at 0.15 pct Mg. At lower concentrations, there is insufficient magnesium for complete oxide disruption and sintering is, therefore, slow. The mechanical properties show similar trends. The ductility is also maximized at 0.15 pct Mg and the change in tensile strength is greatest at this magnesium level. The large increase in strength and ductility at 0.15 pct Mg is a direct consequence of improved interparticle bonding and densification following oxide rupture. The excess magnesium at concentrations >0.15 pct remains in solution in the aluminum, causing expansion by the Kirkendall effect (Figure 1) and solid-solution hardening (Figure 5).

There is one observation, however, which is not entirely consistent with this model. The spinel layer is ~50-nm

thick, whereas the original oxide had a thickness of 50 Å. It is not obvious why the transformation should cause the oxide to coarsen in this way. It is possibly a result of reaction with Mg at the metal-oxide interface and/or between magnesium and any residual oxygen in the atmosphere. Alternatively, shear during compaction may also serve to concentrate the oxide in some regions.

The influence that magnesium has on the sintering of aluminum has important consequences for aluminum powder metallurgy: sintering of aluminum has been considered to be problematical because of the difficulties in wetting the oxide film. Because the oxide can be removed as a sintering obstacle, it allows the design of new alloys. The Al-Sn system is an example. This was considered to have poor sintering characteristics,[46] but this conclusion is only valid in the absence of magnesium.[47] In the extreme, magnesium allows aluminum to be sintered without mechanical compaction, which, in turn, facilitates free-form fabrication and rapid prototyping from aluminum powder.[48] Most aluminum alloys, however, contain magnesium as a separate elemental addition and, therefore, the oxide problem should not exist. This implies that a number of previous investigations need to be re-evaluated.

V. CONCLUSIONS

Trace additions of magnesium powder facilitate the sintering of aluminum by disrupting the oxide film through the formation of spinel ($MgAl_2O_4$). The effect is maximized at <1 wt pct Mg, but this is dependent on the aluminum particle size. Magnesium in the solid state serves a similar purpose in aluminum powder metallurgy to conventional reducing atmospheres in ferrous and cuprous powder metallurgy: it removes the oxide as a barrier to sintering. Magnesium is, therefore, a critical constituent of sintered aluminum alloys.

ACKNOWLEDGMENTS

We thank Comalco Aluminium Ltd., ACL Bearing Company, and Pometon SpA for supplying the metal powder. We also thank Barry Wood and David Page for help with the ESCA and BET measurements, respectively. This work was supported by the Australian Research Council.

REFERENCES

1. R.F. Smart and E.C. Ellwood: *Nature*, 1958, vol. 181, pp. 833-34.
2. R.Q. Guo, P.K. Rohatgi, and D. Nath: *J. Mater. Sci.*, 1997, vol. 32, pp. 3971-74.
3. P. Ramakrishnan and G.S. Tendolkar: *Powder Metall.*, 1964, vol. 7, pp. 34-49.
4. P. Ramakrishnan: *Powder Metall.*, 1966, vol. 9, pp. 47-53.
5. T. Watanabe and Y. Horikoshi: *Int. J. Powder Metall.*, 1976, vol. 12, pp. 209-14.
6. Z.A. Munir: *J. Mater. Sci.*, 1979, vol. 14, pp. 2733-40.
7. Z.A. Munir: *Powder Metall.*, 1981, vol. 24, pp. 177-80.
8. L. Darken and R. Gurry: *Physical Chemistry of Metals*, McGraw-Hill, London, 1953, p. 349.
9. C. Lall: *Int. J. Powder Metall.*, 1991, vol. 27, pp. 315-29.
10. W.D. Kingery: *J. Appl. Phys.*, 1959, vol. 30, pp. 301-06.
11. Ju.V. Naidich: *Prog. Surf. Membr. Sci.*, 1981, vol. 14, pp. 353-484.
12. F. Delannay, L. Froyen, and A. Deruyttere: *J. Mater. Sci.*, 1987, vol. 22, pp. 1-16.
13. S.W. Ip, M. Kucharski, and J.M. Toguri: *J. Mater. Sci. Lett.*, 1993, vol. 12, pp. 1699-1702.
14. Y. Liu, Z. He, S. Yu, G. Dong, and Q. Li: *J. Mater. Sci. Lett.*, 1992, 11, pp. 896-98.
15. D.T. Livey and P. Murray: *Proc. 2nd Plansee Seminar*, 1955, pp. 375-404.
16. J.-G. Li: *Ceramics Int.*, 1994, vol. 20, pp. 391-412.
17. W. Kehl and F. Fischmeister: *Powder Metall.*, 1980, vol. 23, pp. 113-19.
18. M. Humenik Jr and W.D. Kingery: *J. Am. Ceram. Soc.*, 1954, vol. 37, pp. 18-23.
19. R.N. Lumley: Ph.D. Thesis, The University of Queensland, Queensland, 1998.
20. JCPDS–International Centre for Diffraction Data, Newtown Square, PA, 1996
21. G.M. Scamans and E.P. Butler: *Metall. Trans. A*, 1975, vol. 6A, pp. 2055-63.
22. M.J. Couper, M. Nauer, R. Baumann, and R.F. Singer: *Proc. Int. Conf. on PM Aerospace Materials*, Lucerne, Switzerland, Nov. 2–4, 1987.
23. H. Schlich, M. Thumann, and G. Wirth: *Proc. Int. Conf. on PM Aerospace Materials*, Lucerne, Switzerland, Nov. 2–4, 1987.
24. P.E. Doherty and R.S. Davies: *J. Appl. Phys.*, 1963, vol. 34, pp. 619-28.
25. T.B. Sercombe: Ph.D. Thesis, The University of Queensland, Queensland, 1998.
26. *Metals Handbook*, 9th ed., ASM, Metals Park, OH, 1984, vol. 7, pp. 129-30
27. I.A. Shibli and D.E. Davies: *Powder Metall.*, 1987, vol. 30, pp. 97-101.
28. S. Miura, Y. Machida, Y. Hirose and R. Yoshimura: *Proc. 1993 Powder Metallurgy World Congr.*, Kyoto, Japan; appeared in *J. Soc. Powder Powder Metall.*, 1993, pp. 571-74.
29. K. Nishiyama and E. Suzuki: *Proc. 1993 Powder Metallurgy World Congr.*, Kyoto, Japan; appeared in *J. Soc. Powder Powder Metall.*, 1993, pp. 602-05.
30. Y. Nakao, K. Sugaya, S. Seya, and T. Sakuma: U.S. Patent 5,525,292, 1996.
31. A. Kimura, M. Shibata, K. Kondoh, Y. Takeda, M. Katayama, T. Kanie, and H. Takada: *Appl. Phys. Lett.*, 1997, vol. 70, pp. 3615-17.
32. T. Watanabe and K. Yamada: *Int. J. Powder Metall.*, 1968, vol. 4, pp. 37-47.
33. F. Farzin Nia and B.L. Davies: *Powder Metall.*, 1982, vol. 25, pp. 209-15.
34. W.J. Ullrich: *Progress in Powder Metallurgy*, Proc. Conf., MPIF, Princeton, NJ, 1986, vol. 42, pp. 535-56.
35. E.M. Daver, W.J. Ullrich, and K.B. Patel: *Key Eng. Mater.*, 1989, vols. 29-31, pp. 401-28.
36. J.E. Foss and D. DeFranco: SAE Technical Paper No. 940429, SAE, Warrendale, PA, 1994
37. M.W. Chase, Jr., C.A. Davies, J.R. Downey, Jr., D.J. Frurip, R.A. McDonald, and A.N. Syverud: *J. Phys. Chem. Ref. Data*, 1985, Suppl. 1, vol. 14.
38. C.G. Levi, G.J. Abbaschian, and R. Mehrabian: *Metall. Trans. A*, 1978, vol. 9A, pp. 697-711.
39. E. Breval, M.K. Aghajanian, and S.J. Luszcz: *J. Am. Ceram. Soc.*, 1990, vol. 73, pp. 2610-14.
40. R. Molins, J.D. Bartout, and Y. Bienvenu: *Mater. Sci. Eng.*, 1991, vol. A135, pp. 111-17.
41. J. Homeny and M.M. Buckley: *Mater. Lett.*, 1991, vol. 10, pp. 421-24.
42. A. Munitz, M. Metzger, and R. Mehrabian: *Metall. Trans. A*, 1979, vol. 10A, pp. 1491-97.
43. A.D. McLeod and C.M. Gabryel: *Metall. Trans. A*, 1992, vol. 23A, pp. 1279-83.
44. D.H. Kim, E.P. Yoon, and J.S. Kim: *J. Mater. Sci. Lett.*, 1996, vol. 15, pp. 1429-31.
45. N.S. Timofeev and A.P. Savitskii: *Poroshkovaya Metallurgiya*, 1990, No. 3 (327), pp. 188-92.
46. A.P. Savitskii and L.S. Martsunova: *Poroshkovaya Metallurgiya*, 1977, No. 5 (173), pp. 14-19
47. T.B. Sercombe and G.B. Schaffer: *Advances in Powder Metallurgy and Particulate Materials—1997*, Proc. 1997 Conf. on Powder Metallurgy and Particulate Materials, Chicago, IL, June 29–July 2, 1997, R. McKotch and R. Webb, eds., Metal Powder Industries Federation, Princeton, NJ.
48. T.B. Sercombe, G.B. Schaffer, and P. Calvert: unpublished research.